

A Bayesian Approach to Estimate the Capacity Factor of Offshore Wind Farms on the Brazilian Coast

J.F.M. Pessanha

V.A. Almeida

Electric Energy Research
Center (CEPEL)

Rio de Janeiro, Brazil
{francisc.andrade}@cepel.br

A.C.G. Melo

M.E.P. Maceira

Rio de Janeiro State University
(UERJ)

Rio de Janeiro, Brazil
{albert.melo,melvira}@ime.uerj.br

M.J.C. Mendonça

Institute of Applied Economic
Research (IPEA)

Rio de Janeiro, Brazil
mario.mendonca@ipea.gov.br

L.A. Medrano

Federal Rural University of
Rio de Janeiro (UFRRJ)

Seropédica-RJ, Brazil
lmedrano@ufrj.br

Abstract—This work presents a Bayesian approach for inferring the capacity factor of an offshore wind farm. The calculation of the capacity factor depends on the power curve model and the probabilistic wind speed model, which in this work follows a Weibull distribution, whose scale and shape parameters are estimated using a Bayesian approach where the priors are independent gamma distributions, the likelihood is the Weibull distribution, and the posteriors are obtained by Hamiltonian Monte Carlo. The application of the described methodology is illustrated through a case study of an offshore wind power project located on the Northern coast of the Rio de Janeiro State, Brazil.

Index Terms—Bayesian statistics; capacity factor; offshore wind projects; Weibull distribution; wind power.

I. INTRODUCTION

The use of wind energy to generate electricity is one of the main resources available to reduce dependence on fossil fuels that contribute to greenhouse gas emissions and global warming, a fundamental requirement for meeting global commitments with carbon neutrality by 2050. The energy transition towards carbon neutrality and the search for energy security has contributed to the rapid expansion of renewable energies, especially wind energy. According to the most recent edition of the Global Wind Report [1], in global terms, wind power plants installed in 2022 added about 78 GW, increasing installed capacity in wind power plants to 906 GW, an annual growth of around 9%. The expectation is that installed capacity will reach the 2 TW in 2030, most of which will come from the addition of new onshore wind farms, but the opportunities provided by offshore wind farms point to an important contribution of the latter in expanding installed capacity.

The abundance of offshore wind resources makes possible the use of electrolysis to produce hydrogen without the use of fossil fuels, i.e., “green” hydrogen [2]. The hydrogen is considered a promising alternative to fossil fuels, as its combustion only produces water vapor and as hydrogen is a key input in several industries, the green hydrogen has a multiplier effect on decarbonizing the economy. In addition, electrolysis requires water and the possibility of using seawater creates a synergy between offshore wind and hydrogen production.

Although electrolysis with seawater still presents some technological challenges to be overcome [3], offshore wind has attracted several investors, as illustrated by the 74 offshore wind farms projects with environmental licensing processes currently under analysis by the Brazilian Institute for the Environment and Renewable Natural Resources (IBAMA) and that add up a total installed capacity of 182 GW, a small portion of Brazil’s offshore wind potential of around 3 TW and 14,800 TWh of average annual electricity production [4]. It is worth noting that offshore and onshore wind power potentials in Brazil are unlikely to be negatively impacted by global climate change in the future [4]-[6].

The offshore wind farms can span larger areas and exploit winds smoother and faster, free of obstacles and with more powerful turbines [7]. In addition, offshore wind projects are close to load centers - the coastal zone of Brazil concentrates almost a quarter of the population and activities in this range are responsible for approximately 20% of the Brazilian GDP [8]. However, the investment and operating costs of offshore wind farms are higher than their onshore counterparts and the assessment of the wind potential of offshore wind projects is more complex [9],[10].

As Brazil moves towards harnessing its offshore wind potential, accurate capacity factor estimations will play a crucial role in informing investment decisions. Aiming to contribute to the subject, this work presents a case study where a Bayesian approach [11]-[14] was applied to evaluate the capacity factor of an offshore wind project, based on data from the Brazilian Wind Potential Atlas - BWPA [15], wind speed measurements and technical turbine parameters. Importantly, the methods applied in the case study is equally applicable to onshore wind farms.

Furthermore, in contrast to the study in [14], which models the capacity factor of offshore wind farms operating in the United Kingdom, the methodology employed in this case study enables the estimation of the capacity factor for wind farms during the planning phase, when available measurements consist solely of wind speed records. Thus, this study extends beyond the Bayesian estimation of Weibull distribution



parameters [11]-[13], commonly adopted in wind speed modelling [16]. It's noteworthy that traditionally, wind speed frequency distribution modeling follows a classical statistical inference approach to estimate the shape and scale parameters of the Weibull distribution. These parameters, when combined with the power curve of a wind turbine, allow for the estimation of the capacity factor [17],[18].

The Bayesian approach differs from the classical paradigm in its ability to incorporate prior knowledge into the inference process, expressed through prior distributions, and combine it with data using Bayes' theorem. Then the Bayesian approach allow combine previous knowledge about the wind in the region where the wind power project will be sited with local wind speed measurements without the need for long series of wind speed measurements [11]. The resulting posterior distributions provide easily interpretable and useful results for assessing the risks of a wind project, such as credibility intervals for the capacity factor and energy production.

This work is organized into six sections. Next, in section II, some basic concepts about wind energy are presented, with emphasis on the calculation of the capacity factor of a wind power project. In turn, section III presents the basic principles of Bayesian inference. The methodology for evaluating the capacity factor of a wind farm is described in section IV. The application of the described methodology is illustrated in section V through the case study of an offshore wind farm located on the Northern coast of the State of Rio de Janeiro, Brazil, next to important economic hubs [19]. Finally, the main conclusions of the work are presented in section VI.

II. WIND POWER

The relationship between the wind speed v (m/s) and the generated electrical power P (Watts) is determined by the power curve $P(v)$ in Fig. 1, whose mathematical formulation is described in (1), where C_p denotes the coefficient of performance, η_g is the efficiency of the generator, η_m is the efficiency of the transmission box, ρ is the air density (kg/m³), A is the area swept by the rotor (m²), v_{cut-in} , v_{rated} and $v_{cut-out}$ represent the velocity levels of the wind (m/s), i.e., cut-in wind speed, rated wind speed e cut-out wind speed, respectively [18].

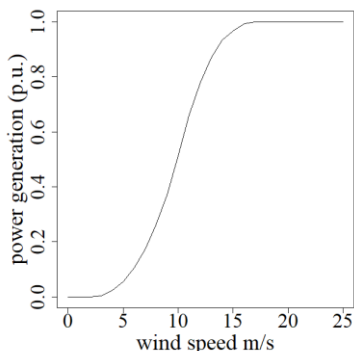


Figure 1. Power curve.

The power curves can be obtained from the turbine catalogs provided by the manufacturers. As illustrated in Fig. 1, power

generation starts with wind speeds above 2 or 3 m/s. The generated power grows with the cube of the wind speed until reaching the rated wind speed, whose value varies between 10 m/s and 17 m/s, depending on the turbine model. For speeds above the v_{rated} , the generated power is close to the rated power, but the turbine is turned off to avoid the risk of damage when the cut-out wind speed is exceeded, e.g., 25 m/s.

$$P(v) = \begin{cases} 0, v \leq v_{cut-in} \\ \frac{1}{2} C_p \eta_m \eta_g \rho A v^3, v_{cut-in} \leq v \leq v_{rated} \\ \frac{1}{2} C_p \eta_m \eta_g \rho A v_{rated}^3, v_{rated} \leq v \leq v_{cut-out} \\ 0, v > v_{cut-out} \end{cases} \quad (1)$$

The maximum (rated) power corresponds to the power achieved at rated wind speed:

$$P_{max} = \frac{1}{2} C_p \eta_m \eta_g \rho A v_{rated}^3 \quad (2)$$

The wind speed v in (1) correspond to the speed at the hub height. In general, the anemometers are installed between 10 m and 50 m above the ground, but through (3) the wind speed measurements v_1 at height h_1 are adjusted to v_2 at the hub height h_2 , whose magnitude can exceed 100 m. For offshore projects, the power exponent α in (3) is fixed at 0.06 [20].

$$v_2 = v_1 \left(\frac{h_2}{h_1} \right)^\alpha \quad (3)$$

Due to its intermittent behavior, the wind speed v can be described by a random variable with Weibull distribution [16],[21], whose probability density function (4) depends on the parameters of scale s and shape k . The expected value of the wind power production is given in (5).

$$f(v) = \frac{k}{s} \left(\frac{v}{s} \right)^{k-1} \exp \left[- \left(\frac{v}{s} \right)^k \right] \quad (4)$$

$$\bar{P} = \int_0^\infty P(v) f(v) dv \quad (5)$$

The capacity factor (CF) is given by the ratio \bar{P}/P_{max} and as demonstrated in [17], can be estimated by (6).

$$CF = \frac{1}{v_{rated}^3} \int_{v_{cut-in}}^{v_{rated}} v^3 f(v) dv + \int_{v_{rated}}^{v_{cut-out}} f(v) dv \quad (6)$$

Note that the CF depends on the scale and shape parameters of the Weibull probability density function $f(v)$, estimated from wind speed data. Under the commonly accepted Rayleigh distribution assumption (Weibull with $k=2$) for wind speed prevalent in Europe, the capacity factor can be estimated by the following nonlinear approximation [22]:

$$CF = (1 - 0.087) \left[\tanh \left(\frac{0.087 \bar{V}^2}{2\pi \left(1 + \frac{P}{D^2} \right) + \frac{P}{2D^2}} \right) \right] - \frac{0.087}{2\pi \bar{V} \left(1 - \frac{P}{D^2} \right)} \quad (7)$$

where \bar{V} represents the average wind speed, P is the nominal power of the turbine, and D denotes the rotor diameter.

As indicated in (8), from the capacity factor it is possible to estimate the energy produced over an interval of T hours by a wind farm composed of N turbines with unit power P .

$$\text{Production} = N \times P \times T \times CF \quad (8)$$

III. BAYESIAN INFERENCE

In the Bayesian approach the unknown parameter θ is modeled by a probability distribution, a clever way to represent the underlying uncertainty. Initially, such distribution, called prior $p(\theta)$, capture the available information about the parameter, but through Bayes' Theorem, it can be updated with data from a random sample with n observations $X=\{x_1, \dots, x_n\}$ in order to achieve a posterior distribution $p(\theta|X)$ [23]:

$$p(\theta|X) = \frac{p(X|\theta)p(\theta)}{p(X)} \quad (9)$$

where $p(X) = \int p(X|\theta)p(\theta)d\theta$.

Given that $p(X)$ is just a normalization constant, then the posterior probability is proportional to the product of the likelihood $p(X|\theta)$ and the prior $p(\theta)$:

$$p(\theta|X) \propto p(X|\theta)p(\theta) \quad (10)$$

From the posterior distribution in (10) we can compute the probability distribution of a new value (x^{new}), i.e., the predictive distribution in (11).

$$p(x^{new}|X) = \int p(x^{new}|X, \theta)p(\theta|X)d\theta \quad (11)$$

The choice of a prior distribution is an important step in the Bayesian approach. In the case of the Weibull distribution, there are some options for choosing the prior distribution, among them the gamma-gamma model [12], in which the priors for the scale and shape parameters are modeled by independent gamma distributions [13], whose probability density functions are presented in (12) and (13):

$$s \sim \text{gamma}(\alpha_1, \beta_1) \rightarrow p(s) = \frac{\beta_1^{\alpha_1}}{\Gamma(\alpha_1)} s^{\alpha_1-1} e^{-\beta_1 s} \quad (12)$$

$$k \sim \text{gamma}(\alpha_2, \beta_2) \rightarrow p(k) = \frac{\beta_2^{\alpha_2}}{\Gamma(\alpha_2)} k^{\alpha_2-1} e^{-\beta_2 k} \quad (13)$$

It is worth noting that the core of the Rayleigh distribution (Weibull with $k=2$) is a gamma distribution, in this case the prior and the posterior are gamma distributions [24], i.e., they are conjugated.

The hyperparameters α and β in (12) and (13) are determined from information about the scale and shape parameters from BWPA [15]. In a gamma distribution, the mean is α/β and the variance is α/β^2 , but for the purposes of determining the hyperparameters of a prior, it can be admitted

that β is inversely proportional to α , i.e., $\beta=1/\alpha$. Thus, from the estimates provided by the wind atlas (\hat{s} and \hat{k}), the hyperparameters can be determined by the method of moments, as shown in Table I.

TABLE I. COMPUTATION OF PRIOR HYPERPARAMETERS

Prior	Hyperparameters	
	α	β
gamma(α_1, β_1)	$\alpha_1 = \sqrt{\hat{s}}$	$\beta_1 = 1/\sqrt{\hat{s}}$
gamma(α_2, β_2)	$\alpha_2 = \sqrt{\hat{k}}$	$\beta_2 = 1/\sqrt{\hat{k}}$

For a set $\{x_1, \dots, x_n\}$ with n records sampled from a Weibull(s, k) distribution, the likelihood is given by (14).

$$p(x|s, k) = \frac{k^n}{s^{nk}} \prod_{i=1}^n (x_i)^{k-1} e^{-\sum_{i=1}^n \left(\frac{x_i}{s}\right)^k} \quad (14)$$

Then, the posterior distribution is proportional to the product of the likelihood in (14) by the priors in (12) and (13):

$$p(s, k|x) \propto \frac{k^{n+\alpha_2-1}}{s^{nk-\alpha_1+1}} \prod_{i=1}^n (x_i)^{k-1} e^{-\sum_{i=1}^n \left(\frac{x_i}{s}\right)^k - \beta_1 s - \beta_2 k} \quad (15)$$

The posterior joint distribution of (s, k) in (15) cannot be analytically treated when the objective is to obtain the marginal distributions of s and k . However, the marginal distributions can be obtained by applying the Gibbs sampler through the conditional density functions (16) and (17) [24].

$$p(s|x, k) \propto \frac{1}{s^{nk-\alpha_1+1}} e^{-\sum_{i=1}^n \left(\frac{x_i}{s}\right)^k - \beta_1 s} \quad (16)$$

$$p(k|s, x) \propto \frac{k^{n+\alpha_2-1}}{s^{nk}} e^{k \sum_{i=1}^n \ln(x_i) - \sum_{i=1}^n \left(\frac{x_i}{s}\right)^k - \beta_2 k} \quad (17)$$

In this work we applied the Hamiltonian Monte Carlo - HMC [25] instead of the Gibbs sampler. The HMC is available in the rstan [26] and just as the Gibbs sampling, it is a method of Markov Chain Monte Carlo - MCMC. However, the HMC method is more efficient than the Gibbs Sampling [25]. The posterior predictive distribution is given by the following double integral:

$$p(x^{new}|x) = \iint p(x^{new}|s, k)p(s, k|x)dsdk \quad (18)$$

IV. CAPACITY FACTOR MODELING

From the posterior distributions in (15), (16) and (17) one can sample pairs of (scale factor s , shape factor k) and introduce them into (6) to compute the respective capacity factor (CF). As shown in Fig. 2, at the end of this process the probability distribution of the capacity factor is achieved. From the distribution of the capacity factor, it is possible to compute the average or median capacity factor of the offshore wind farm project and the respective credibility interval.

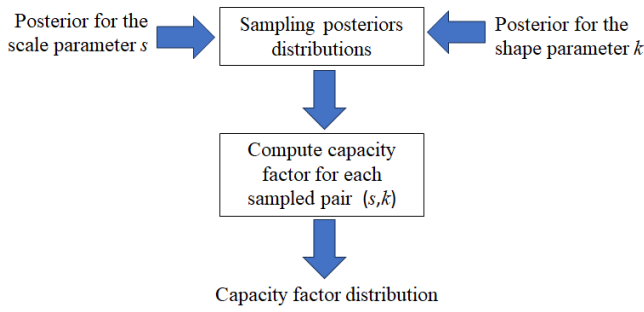


Figure 2. Simulation to estimate the probability distribution of the CF.

V. CASE STUDY

To illustrate the application of the described methodology, consider the offshore wind project RJ-04 located about 41 km away from the city of Armação dos Búzios – RJ, Brazil, more precisely at coordinates 22°38'22"S and 41°28'59"W, the location indicated by the blue circle on the map of Brazil in Fig. 3. The offshore wind farm will have 188 turbines of 15 MW each, leading to a total installed capacity of 2,820 MW. In this case study, the wind turbines correspond to the reference model with a capacity of 15 MW from the International Energy Agency (IEA) with a rotor of 240 m, hub height at 150 m above sea level and speeds $V_{cut-in}=3$ m/s, $V_{rated}=10.59$ m/s and $V_{cut-out}=25$ m/s [27]. Annual estimates of scale and shape factors at 100 m height (onshore) in the vicinity of the wind farm can be obtained from the BWPA (Table II).



Figure 3. Location of the offshore wind farm project RJ-04.

TABLE II. SCALE AND SHAPE ESTIMATES FROM BWPA

Coordinates	Armação dos Búzios 22°44'17"S, 41°52'20"W
scale factor (m/s)	$s = 8.5$
shape factor	$k = 2.4$

The application of the described methodology is preceded by the adjustment of the estimates of the scale and shape factors for the hub height, in this case 150 m. The adjusted estimates \hat{s} and \hat{k} presented in Table III are obtained through (19) and (20), where h_1 is the reference height of the estimates (in this case 100 m) and h_2 is the hub height [21].

$$s_{h_2} = s_{h_1} \left(\frac{h_2}{h_1} \right)^n \quad (19)$$

$$k_{h_2} = k_{h_1} \left[\frac{1 - 0.088 \times \ln(h_1/10)}{1 - 0.088 \times \ln(h_2/10)} \right] \quad (20)$$

where

$$n = \frac{0.37 - 0.088 \times \ln(s_{h_1})}{1 - 0.088 \times \ln(h_1/10)} \quad (21)$$

TABLE III. ADJUSTED SCALE AND SHAPE ESTIMATES

Parameters	Adjusted Estimates
scale	$\hat{s} = 9.3227$
shape (m/s)	$\hat{k} = 2.5124$

Inserting the estimates presented in Table III into the formulas shown in Table I, we obtain the hyperparameters of the priors illustrated in Fig. 4.

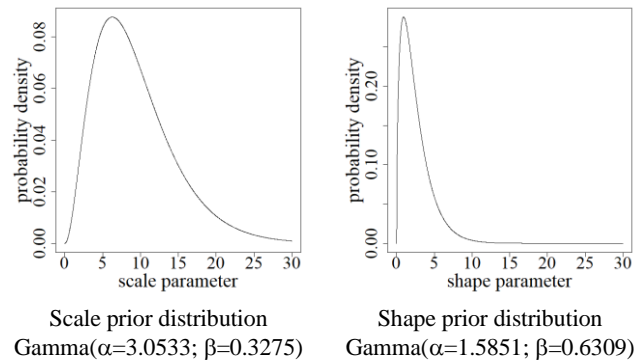


Figure 4. Priors for scale and shape parameters.

In the absence of wind speed measurements for the location of the RJ-04 wind farm project, we considered the hourly data from the Cabo Frio 2 buoy maintained by the National Buoy Program (PNBOIA) and located at coordinates 23°37'47.28"S and 42°12'10.08"W, 132 km away from the RJ-04 wind farm.

The Cabo Frio 2 buoy has two anemometers located at 4.7 m and 3.7 m above the sea surface. The wind speed records were adjusted for 150 m height using (3) with $h_T=4.7$ m and power exponent equal to 0.06 [20]. The buoy was launched in June, 2016 and was collected in November, 2018. For the case study, the 8,751 hourly records comprising the period between August 1, 2016 and July 31, 2017 were considered, whose histogram, adjusted for 150 m, is shown in Fig. 5.

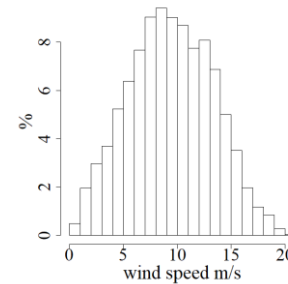


Figure 5. Wind speed records from Cabo Frio 2 buoy adjusted to 150 m.

The computational implementation of the described methodology was carried out by the rstan package [26] for R environment [28]. Thus, from the priors presented in Fig. 4 and the wind speed measurements in Fig. 5, the Hamiltonian Monte Carlo [25] was applied to obtain the posterior distributions of the scale and shape parameters. Four Markov chains (the default setting of the rstan R package) with 5,000 iterations of the MCMC algorithm were executed as shown in Fig. 6, for the purpose of assessing convergence (2500 warmup samples).

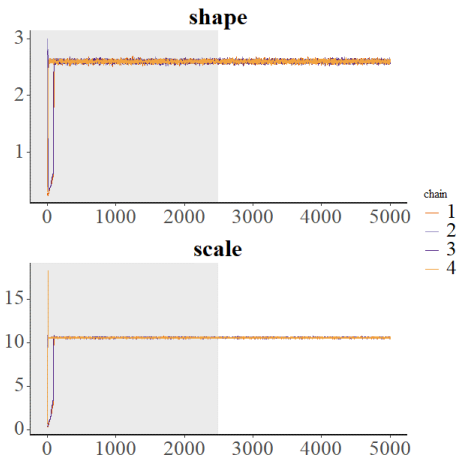


Figure 6. MCMC Simulation Convergence.

The histograms of the posterior distributions are illustrated in Fig. 7 and Fig. 8. From these distributions we achieved the 95% credibility intervals [10.47, 10.65] and [2.56, 2.64] for scale and shape parameters respectively.

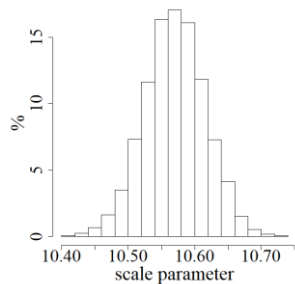


Figure 7. Posterior of the scale parameter s .

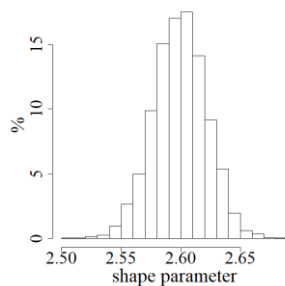


Figure 8. Posterior of the shape parameter k .

The posterior predictive distribution of wind speed is presented in Fig. 9. Sampling the posteriors of the scale and shape parameters and substituting in (6) we obtain the distribution of the capacity factor depicted in Fig. 10, whose median is 0.6066, a value compatible with the estimated capacity factor of 60% for the wind turbine adopted in the RJ-04 project.

The application of the described procedure for each month of the year produced the results presented in Table IV, that include the mean values and the credible intervals of 95% (CI 95%) for shape and scale parameters of the wind speed distributions at 150 m height. The monthly estimates of the capacity factor and energy production from a wind turbine of 15 MW are presented in Table V. Based on (8), the annual energy production for the offshore wind farm RJ-04 (188 wind turbines of 15 MW) is estimated in 14,970 GWh with CI 95% between 14,790 GWh and 15,153 GWh, as shown in Table VI.

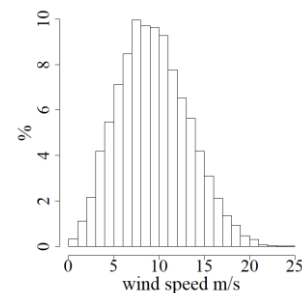


Figure 9. Distribution of wind speed.

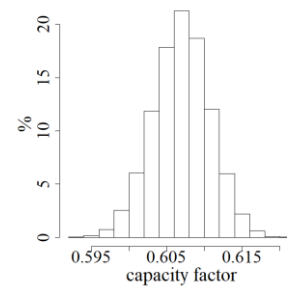


Figure 10. Capacity factor distribution.

TABLE IV. SCALE AND SHAPE POSTERiors FOR 150 M HEIGHT

Months	Shape			Scale		
	Mean	2.5%	97.5%	Mean	2.5%	97.5%
Jan	2.64	2.49	2.80	11.45	11.13	11.78
Feb	3.08	2.89	3.28	10.60	10.33	10.87
Mar	2.55	2.40	2.70	9.23	8.97	9.50
Apr	2.43	2.29	2.57	9.52	9.23	9.81
May	2.40	2.27	2.54	10.66	10.33	11.00
Jun	2.68	2.53	2.83	9.71	9.43	9.99
Jul	3.69	3.47	3.91	10.85	10.63	11.08
Aug	2.69	2.53	2.85	11.42	11.10	11.74
Sep	2.57	2.43	2.72	10.02	9.72	10.32
Oct	2.90	2.73	3.06	11.27	10.98	11.57
Nov	2.25	2.12	2.38	10.99	10.62	11.36
Dec	2.34	2.20	2.48	10.04	9.72	10.37
Annual	2.60	2.55	2.64	10.57	10.48	10.66

TABLE V. CAPACITY FACTOR AND WIND ENERGY PRODUCTION

Months	Capacity Factor Quantiles			Quantiles of Energy Production (GWh) from a turbine of 15 MW		
	2.5%	50%	97.5%	2.5%	50%	97.5%
Jan	0.6398	0.6656	0.6905	7.14	7.43	7.71
Feb	0.6108	0.6367	0.6622	6.16	6.42	6.67
Mar	0.4773	0.5016	0.5263	5.33	5.60	5.87
Apr	0.4951	0.5207	0.5463	5.35	5.62	5.90
May	0.5739	0.5999	0.6260	6.41	6.70	6.99
Jun	0.5208	0.5463	0.5715	5.63	5.90	6.17
Jul	0.6645	0.6879	0.7105	7.42	7.68	7.93
Aug	0.6412	0.6671	0.6921	7.16	7.44	7.72
Sep	0.5399	0.5399	0.5924	5.83	5.83	6.40
Oct	0.6473	0.6722	0.6965	7.22	7.50	7.77
Nov	0.5800	0.6074	0.6336	6.26	6.56	6.84
Dec	0.5283	0.5546	0.5808	5.90	6.19	6.48
Annual	0.5993	0.6066	0.6140	78.67	79.63	80.60

TABLE VI. ANNUAL ENERGY PRODUCTION OF THE WIND FARM RJ-04

Quantiles of the Annual Energy Production (GWh)		
2.5%	50%	97.5%
14,790	14,970	15,153

In order to test the robustness of the results, other sets of priors for the scale and shape parameters were investigated. This was done by maintaining the gamma distribution for the shape parameter but varying the distribution of the scale parameter. The following pairs of distributions were evaluated: (gamma, exponential) and (gamma, lognormal). However, it is worth mentioning that the results did not undergo significant changes due to the use of this set of alternative priors. For brevity, we will not present the results.

For comparison purposes, Table VII displays the capacity factor estimates from alternative approaches.

TABLE VII. CAPACITY FACTOR ESTIMATES FROM OTHER APPROACHES.

Methods	Assumptions	Estimates
The same approach described in this work, but with reanalysis data.	Likelihood calculated with reanalysis	Median = 57% CI 95% (56.3%, 57.7%)
Estimator in (7) with nominal power turbine $P=15000$ kW and rotor diameter $D=240$ m	Average wind speed $\bar{V}=9,4$ m/s (buoy data)	55.4%
	Average wind speed $\bar{V}=8,75$ m/s (reanalysis data)	49.7%
Estimator in (6) with $V_{cut-in}=3$ m/s, $V_{rated}=10.59$ m/s, $V_{cut-out}=25$ m/s and $v\sim$ Weibull(s,k)	Parameters estimated from buoy data ($\hat{\beta}=10.9$ and $\hat{k}=2.59$)	60.8%
	Parameters estimated from reanalysis ($\hat{\beta}=9.78$ and $\hat{k}=3.16$)	57.2%

In Table VII, the first approach uses the same Bayesian methodology employed in this work but with reanalysis data from MERRA 2 provided by <https://www.renewables.ninja/> [29] for the location of wind project RJ-04. Reanalysis data integrate historical observations into a numerical weather prediction model to reconstruct climate, providing a complete spatiotemporal dataset. It's worth noting that a correction was made to the wind speed reanalysis series for the turbine's hub

height, in this case, 150 m. The second approach [22] assumes a Rayleigh distribution for wind speed. This assumption is reasonable for the European continent but lacks empirical support in the Brazilian case. The third alternative [17] utilizes (6) with parameters s and k estimated by the method of moments [18], a classical statistical inference approach.

The results show that the estimates using velocity measurements from the Cabo Frio 2 buoy are higher than the estimates from MERRA2 reanalysis. The capacity factor estimates using reanalysis data reached close to 57%, while the estimates obtained from the Cabo Frio 2 buoy data achieved a capacity factor of 60%. The lowest capacity factor estimates (49.7% and 55.4%) were obtained by the approximation that assumes a Rayleigh distribution for wind speed, and for this reason, they should be viewed with caution in the Brazilian context.

These capacity factor estimates are in line with projections from the International Renewable Energy Agency (IRENA), which indicate a range between 36% and 58% for offshore wind capacity factors in 2030 and between 43% and 60% in 2050 [30]. In addition, although measurements and reanalysis data are used in the case study, the described methodology can be applied to projections coming from general circulation models, to capture the impact of the global climate change on future wind patterns, e.g., RegCM4 [31] or CMIP5 [32].

VI. CONCLUSIONS

The Bayesian based approach pointed to be useful in the evaluation of the capacity factor or the energy production of a wind power project, once from the statistics available in an atlas of wind potential it is possible to formulate prior distribution that represent the prior knowledge about the wind regime to be explored, that can be combined with site wind speed measurements. Furthermore, the existence of a prior distribution allows good inferences to be made even with small samples, as in the case study carried out which had only 1 year of hourly anemometric records. The posterior distribution provides results that are easy to interpret and useful for risk assessment of a wind power project, e.g., the credible intervals for the capacity factor and energy production. In the case study presented, measurements of offshore wind speed were considered at a point 132 km away from the evaluated wind project and containing only one year of hourly records. Despite these limitations, the results obtained were satisfactory and the estimates obtained for the capacity factor are compatible with the projections from IRENA and the estimate informed by the wind turbine manufacturer considered in the evaluated wind power project.

REFERENCES

- [1] GWEC – Global Wind Energy Council. “Global Wind Report,” Mar. 2023. Available: https://gwec.net/wp-content/uploads/2023/04/GWEC-2023_interactive.pdf
- [2] A. Kumar, F. Khan, and R. Dudhe. “A Review of Green Hydrogen for Economical and Feasible Alternate Aligning with net-zero,” in *Proc. 2023 Advances in Science and Engineering Technology International Conferences (ASET)*, Dubai, United Arab Emirates, pp. 1-7, Available: doi: 10.1109/ASET56582.2023.10180439.



- [3] R.R. Beswick, A.M. Oliveira, and Y. Yan, "Does the Green Hydrogen Economy Have a Water Problem?," *ACS Energy Letters*, 6, pp. 3167-3169, 2021.
- [4] S.S.P. Azevedo, A.O. Pereira Junior, N.F. Silva, R.S.B. Araújo, and A.A. Carlos Júnior "Assessment of offshore wind power potential along the Brazilian coast," *Energies*, 13, 2557, 2020. Available: <https://doi.org/10.3390/en13102557>.
- [5] A.F.P. Lucena, A.S. Sklo, R. Schaeffer, and R.M. Dutra, "The vulnerability of wind power to climate change in Brazil," *Renewable Energy*, v. 35, n. 5, pp. 904-912, May 2010.
- [6] E.B. Pereira, F.R. Martins, M.P. Pes, E. I. Cruz Segundo, and A.A. Lyra, "The impacts of global climate changes on the wind power density in Brazil," *Renewable Energy*, v. 49, pp. 107-110, Jan. 2013.
- [7] H. Li, C. Guedes Soares, "Reliability analysis of floating offshore wind turbines support structure using Hierarchical Bayesian Network," in *Proc. 29th European Safety and Reliability Conference*, Hannover, Germany, Sep. 2019.
- [8] I.O. Andrade, G.R.L. Hillebrand, T. Santos, T.C.F. Mont'Alverne, and A.B. Carvalho, "Brazilian maritime GDP, social economic and environmental motivations for its measurement and monitoring," Institute for Applied Economic Research, Brasília, DF, Discussion paper 265, Mar. 2022.
- [9] B. Desalegn, D. Gebeyehu, B. Tamrat, T. Tadiwose, and A. Lata, "Onshore versus offshore wind power trends and recent study practices in modeling of wind turbines' life-cycle impact assessments," *Cleaner Engineering and Technology*, 17, 100691, Dec. 2023.
- [10] X. Ma, Y. Liu, J. Yan, S. Han, L. Li, H. Meng, M. Deveci, K. Kolle, and U. Cali, "Assessment method of offshore wind resource based on a multi-dimensional indexes system," *Journal of Power and Energy Systems*, v. 10, pp. 76-87, Jan. 2024.
- [11] M.G.M. Khan, M.R. Ahmed, "Bayesian method for estimating Weibull parameters for wind resource assessment in the Equatorial region: a comparison between two-parameter and three-parameter Weibull distributions." *Research Square*, 2022.
- [12] M. Aslam, S. M. A. Kazmi, I. Ahmad, and S. H. Shah, "Bayesian estimation for parameters of the Weibull distribution," *Science International (Lahore)*, 26(5), 1915-1920, 2014.
- [13] E.F. Saraiva, A.K. Suzuki, "Bayesian computational methods for estimation of two parameters Weibull distribution in presence of right-censored data," *Chilean Journal of Statistics*, v. 8, n. 2, pp. 25-43, Sep. 2017.
- [14] D. Wilkie, C. Galasso, "A Bayesian model for wind farm capacity factors," *Energy Conversion and Management*, 252, 114950, 2022.
- [15] C.B. Neiva, R.M. Dutra, S.R.F.C. Melo, V. G. Guedes, A.A.M. Cabrera, W.G. Almeida, and R.O. Braz, "Brazilian Wind Energy Potential Atlas: Simulations 2013," Centro de Pesquisas de Energia Elétrica, Rio de Janeiro, 2017.
- [16] C.G. Justus, W.R. Hargraves, A. Mikhail, D. Graber, "Methods for Estimating Wind Speed Frequency Distributions," *Journal of Applied Meteorology*, v. 17, 350-353, Mar.1978.
- [17] S.H.J. Jangamshetti, V.G. Rau, "Site matching of wind turbine generators: a case study," *IEEE Transactions on Energy Conversion*, v. 14, no. 4, pp. 1537-1543, Dec. 1999.
- [18] J.F.M. Pessanha, F.L.C. Oliveira, and R.C.Souza, "Teaching statistical methods in engineering courses through wind power data," in *Proc. 2015 IASE Satellite Conference*, Rio de Janeiro.
- [19] T.R. Coriolano, N.T. Signorelli, J. Lugon Junior, M.A.C. Moreira, and M.G.A.J. Silva, "Study of the temporal variation of offshore wind energy potential in Southeast Brazil," *Ciência e Natureza*, v. 44, 2022, Available: <https://doi.org/10.5902/2179460X668814>
- [20] A.M. Olsen, M. Øiestad, E. Berge, M.Ø. Køltzow, T. Valkonen, "Evolution of Marine Wind Profiles in the North Sea and Norwegian Sea Based on Measurements and Satellite-Derived Wind Products," *Tellus A: Dynamic Meteorology and Oceanography*, 74, pp. 1-16, 2022.
- [21] Y. Ding, *Data Science for Wind Energy*, Boca Raton, FL: CRC Press, 2020.
- [22] Y. Ditkovich, A. Kuperman, "Comparison of three methods for wind turbine capacity factor estimation," *The Scientific World Journal*, Article 805238, 2014, Available: <https://doi.org/10.1155/2014/805238>.
- [23] J.V. Stone, *Bayes' Rule: A tutorial introduction to Bayesian analysis*, Sebel Press, 2013.
- [24] M.A.A. Turkman, C.D. Paulino, *Computational Bayesian Statistics: A Introduction*, (In Portuguese), Sociedade Portuguesa de Estatística. Lisbon, 2015.
- [25] O. A. Martin, R. Kumar, and J. Lao, *Bayesian Modeling and Computation in Python*, Boca Raton, FL: CRC Press, 2022.
- [26] B. Carpenter, A. Gelman, M.D. Hoffman, D. Lee, B. Goodrich, M. Betancourt, M. Brubaker, J. Guo, P. Li, and A. Riddell, "Stan: A Probabilistic Programming Language," *Journal of Statistical Software*, 76(1), pp. 1-32, 2017.
- [27] E. Gaertner, J. Rinker., L. Sethuraman, F. Zahle, B. Anderson, G.E. Barter, N.J. Abbas, F. Meng, P. Bortolotti, W. Skrzypinski, G.N. Scott, R. Feil, H. Bredmose, K. Dykes, M. Shields, C. Allen, A. Viselli, "Definition of the IEA 15-Megawatt Offshore Reference Wind Turbine," National Renewable Energy Laboratory, Golden, CO, Tech. Rep. NREL/TP-5000-75698, 2020.
- [28] R Core Team, R: A language and environment for statistical computing. R Foundation for Statistical Computing, Vienna, 2021, Available: <https://www.R-project.org/>.
- [29] I. Staffell, S. Pfenninger, "Using bias-corrected reanalysis to simulate current and future wind power output," *Energy*, v. 114, 1, pp. 1224-1239, Nov. 2016.
- [30] IRENA, Future of Wind: Deployment, Investment, Technology, Grid Integration and Socio-Economic Aspects (A Global Energy Transformation Paper). International Renewable Energy Agency, Abu Dhabi (n.d.), 2019.
- [31] J. Wu, Z.Y. Han, Y.P. Yan, C.Y. Sun, Y. Xu, Y. Shi, "Future changes in wind energy potential over China using RegCM4 under RCP emission scenarios," *Advances in Climate Change Research*, v. 12, 4, pp. 596-610, Aug. 2021.
- [32] D. Carvalho, A. Rocha, M. Gómez-Gesteira, C. Silva Santos, "Potential impacts of climate change on European wind energy resources under the CMIP5 future climate projections," *Renewable Energy*, 101, pp. 29-40, Feb. 2017